

## Cyanide Spectroscopy in Laser-Induced Plasma

CHRISTOPHER M. HELSTERN<sup>1</sup>, CHRISTIAN G. PARIGGER<sup>1\*</sup>, BENJAMIN S. JORDAN<sup>2</sup>,  
DAVID M. SURMICK<sup>3</sup>, ROBERT SPLINTER<sup>4</sup>

<sup>1</sup>Physics and Astronomy Department, University of Tennessee, University of Tennessee Space Institute,  
Center for Laser Applications, 411 B.H. Goethert Parkway, Tullahoma, TN 37388-9700, USA

<sup>2</sup>Nuclear Engineering Department, University of Tennessee, Tickle College of Engineering,  
1412 Circle Drive, Knoxville, TN 37912, USA

<sup>3</sup>Physics and Applied Physics, University of Massachusetts Lowell, Lowell, MA 01854, USA

<sup>4</sup>Welling Medical, Van der Waals Park 22, 9351 VC Leek, The Netherlands

\*Corresponding author E-mail: cparigge@tennessee.edu (C.G. Parigger)

**ABSTRACT:** This article reports new measurements of laser-induced plasma of diatomic molecular cyanide (CN). Focused, high-peak power, 1.064-nm Q-switched radiation of the order of 1 TW/cm<sup>2</sup> generates optical breakdown plasma in a cell at pressures of  $3.04 \times 10^5$  Pascal. Line-of-sight analysis of recorded molecular spectra indicate the outgoing shockwave at expansion speeds well in excess of Mach number 5. Spectra of atomic carbon confirm an increased electron density near the shock wave, and equally, molecular CN spectra reveal higher excitation temperature near the shockwave.

**PACS Codes:** 52.70.-m, 33.20.-t, 52.25.Jm, 42.62.Fi

**Keywords:** Plasma diagnostics, molecular spectra, plasma spectroscopy, laser spectroscopy, laser-induced breakdown spectroscopy.

### 1. INTRODUCTION

Cyanide (CN) spectra produced from molecular recombination spectra are observed following optical breakdown in gases for time delays of the order of 100 ns after the end of the laser pulse [1]. CN plasma dynamics are observed by using gas mixtures. Applications of cyanide spectroscopy include potential medical and forensic applications.

Cyanide poisoning can cause detrimental effects and possible death. Symptoms include dizziness, shortness of breath, vomiting, seizures, loss of consciousness, and cardiac arrest [2]. Even if an individual survives a substantial intake of cyanide, there can be long-term consequences such as ones associated with neurological problems [3]. Human exposures are typically seen from house fires or from workplaces involved in pesticide and plastic manufacturing [4]. Routes of intake can occur via inhalation, ingestion, and absorption through the skin. Additionally, cyanide poisoning diagnosis is difficult [2] and testing is either fairly time consuming or subject to false positives (e.g., colorimetric assays) [5]. Therefore, it is a necessary to have an effective method to determine cyanide poisoning.

Forensic investigations are necessary for deaths associated with acute cyanide poisoning. Normal blood cyanide concentrations are 0.25  $\mu\text{gD mL}$  or lower, and concentrations between 0.25 and 2–3  $\mu\text{g/mL}$  are defined as elevated, but not associated with causing death. Death due to cyanide poisoning in absence of other relevant toxicological findings are associated with cyanide blood concentrations of 3  $\mu\text{gD mL}$  and above [6]. Due to bacteriological activity in blood samples cyanide instability arises as time elapses. [7]. Additionally, samples taken from mouth and nose must be evaluated in a couple days otherwise the elevated cyanide levels will be non-detectable using current toxicological testing. [8] Therefore, it is imperative to have an efficient means of detecting cyanide concentrations quickly.

## 2. EXPERIMENTAL DETAILS

The standard experimental components are used for laser-induced breakdown spectroscopy and have been summarized previously, e.g., see Ref. [1], but are included for completeness. The experimental arrangement consists of a set of components typical for time-resolved, laser-induced optical emission spectroscopy, or nanosecond laser-induced breakdown spectroscopy (LIBS) [9]. Primary instrumentations include a Q-switched Nd:YAG device (**Quantel model Q-smart 850**) operated at the fundamental wavelength of 1064-nm to produce full-width-at-half-maximum 6-ns laser radiation with an energy of 850 mJ per pulse, a laboratory type Czerny-Turner spectrometer (Jobin Yvon model HR 640) with a 0.64 m focal length and equipped with a 1200 grooves/mm grating, an intensified charge coupled device (Andor Technology model iStar DH334T-25U-03) for recording of temporally and spatially resolved spectral data, a laboratory chamber or cell with inlet and outlet ports together with a vacuum system, electronic components for synchronization, and various optical elements for beam shaping, steering and focusing. Figure 1 displays the principal schematic of the experimental arrangement. The laser beam is focused into the cell held at a pressure of approx. 3 atmospheres.

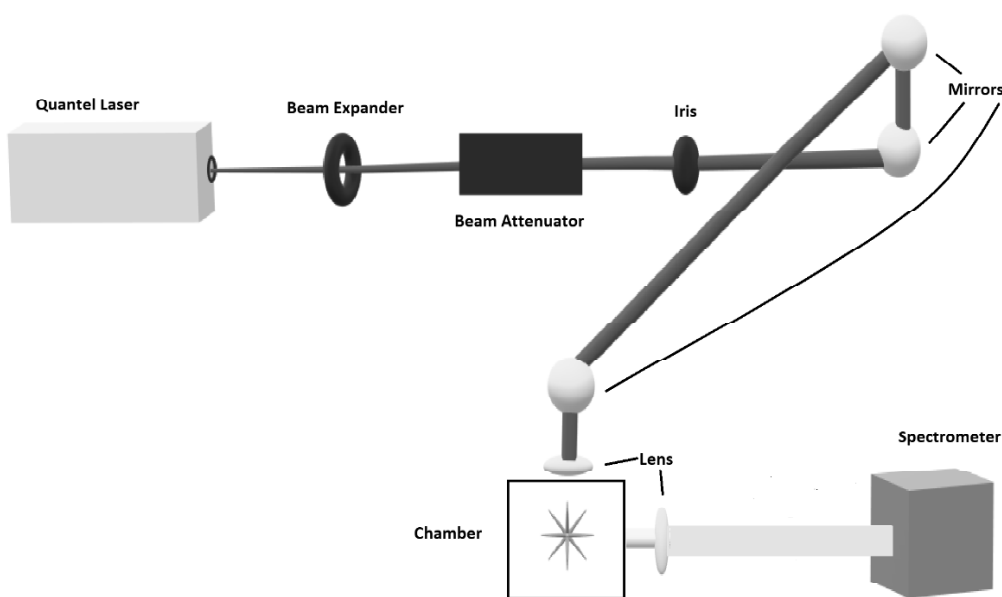


**Figure 1: Modular schematic of laser-induced breakdown experiment.**

For the generation of optical breakdown micro-plasma, a singlet lens (Thorlabs model LA1509-C) is used close to the top entrance window of one arm of the chamber containing the 1:1 CO<sub>2</sub>:N<sub>2</sub> gas mixture held at  $3.04 \times 10^5$  Pascal (Airgas ultra-high purity N<sub>2</sub> and research grade CO<sub>2</sub>). For 1:1 imaging of the plasma onto the 100 μm spectrometer slit, a fused silica plano-convex lens (Thorlabs model LA4545) is employed. For the CN experiments reported here, the laser pulse energy is attenuated with beamsplitters and apertures from 850 to 200 mJ/pulse.

## 3. RESULTS AND DISCUSSION

The experimental series for the measurement of the CN molecular distribution after optical breakdown includes evacuating the cell to a nominal backing pump pressure of the order of 1 Pa ( $10^{-2}$  Torr), followed by generating the mixture from ultra-high pure N<sub>2</sub> and research grade CO<sub>2</sub>. Optical breakdown was generated inside the chamber at a rate of 10 Hz, with the laser beam focused with f/5 optics from the top, or parallel to the slit. The detector pixels are binned in 4 tracks along the slit direction, resulting in obtaining 256 spectra for each time delay. Recording of measurements consist of 100 accumulations collected for 21 time delays at 250 ns steps. Figures 2 illustrate recorded spatio-temporal spectra that were recorded along the line-of-sight and are accumulated over 100 individual laser-plasma events and the CI 193.09 nm atomic carbon line as identified in previous work [10].

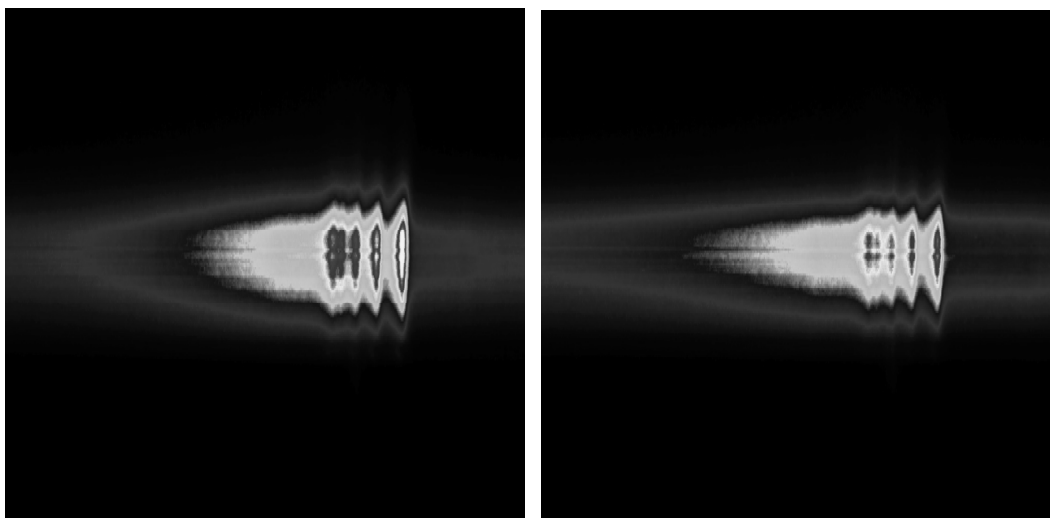


Figure 2: Raw optical breakdown CN-spectra in a 1:1 molar  $\text{CO}_2:\text{N}_2$   $3.04 \times 10^5$  Pa gas mixture for 700 ns (left) and 1200 ns (right) time delays, recorded with 125 ns spectrometer-detector gatewidths.

Figure 3 exhibits result of the analysis of the line-of-sight molecular CN-spectra. The figures reveal the occurrence of the outgoing shockwave along with temperature variations in the central region of the plasma as indicated in previous work [10-12]. These data of slit-height vs. temperature show increased temperature near the edges.

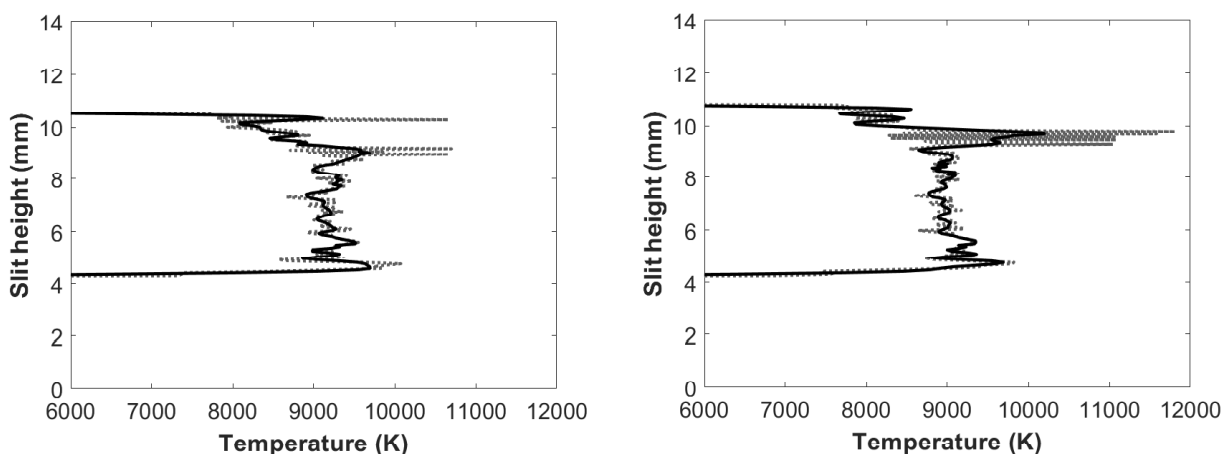


Figure 3: Temperature vs. slit height for CN-spectra (left) 700 ns (right) 950 ns time delay.

The electron number density,  $n_e$ , can be determined from the Stark shift,  $\delta\lambda_{Stark}$ , of the C I 193.09-nm atomic carbon line [13] measured in 2<sup>nd</sup> order,

$$\delta\lambda_{Stark} = d n_e (10^{17} \text{cm}^{-3}), \quad (2)$$

where the shift parameter,  $d$ , is extrapolated [13, 14] to amount to  $d \approx 0.00294$  nm.

Figures 4 display the calculated electron densities versus slit height. The calculated electron densities are of the order of  $n_e \sim 10^{17} \text{cm}^{-3}$  in the central region. Higher electron densities are seen near the edges of the plasma, while smaller electron densities are near the center of the plasma.

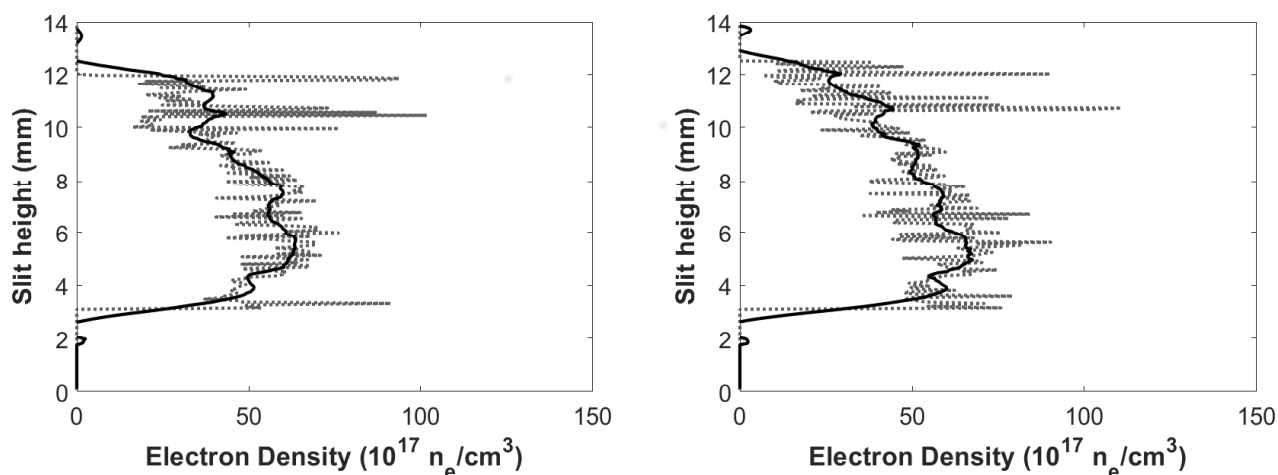


Figure 4: Calculated electron densities versus slit height for time delays of (left) 700 ns and (right) 950 ns.

### 3. CONCLUSIONS

Measurements of recombination CN-spectra at within the first microsecond yields results as expected from atomic hydrogen, Balmer series laser spectroscopy. The analysis indicates higher electron and higher CN-excitation temperature for CN held at  $3.04 \times 10^5$  Pa near the shockwave than in the central region for time delays of the order of one microsecond. The expansion characteristics are deduced from a systematic analysis of the recorded line-of-sight spectra.

#### Acknowledgments

Three of us (CMH, CGP, BSJ) thank for support in part by the Center for Laser Applications at the University of Tennessee Space Institute.

#### References

- [1] C.G. Parigger, C.M. Helstern, G. Gautam, *Int. Rev. At. Mol. Phys.* **8** (2017) 25.
- [2] K. Anseeuw, N. Delvau, G. Burillo-Putze, F. De Iaco, G. Geldner, P. Holmström, Y. Lambert, M. Sabbe, *Eur. J. Emerg. Med.* **20** (2013) 2.
- [3] C.P. Holstege, G.E. Isom, M.A. Kirk, *Goldfrank's Toxicologic Emergencies 8<sup>th</sup> Edition*, Mc-Graw-Hill, USA, 2006.
- [4] N. Gupta, Balomajumder, V.K. Agarwal, *J. Hazard. Mater.* **176** (2010) 1.
- [5] N.T. Lappas, C.M. Lappas, *Forensic Toxicology: Principles and Concepts 1<sup>st</sup> Edition*, Academic Press, USA, 2016
- [6] V. Gambaro, S. Arnoldi, E. Casagni, L. Dell'Acqua, C. Pecoraro, R. Frodli, *J. Forensic Sci.* **52** (2007) 1401.
- [7] A. Surleva, R. Gradinaru, G. Drochioiu, *International Journal of Criminal Investigation* **2** (2012) 79.
- [8] S.Y. Li, I. Petrikovics, J. Yu, *Forensic Sci. Rev.* **31** (2019) 45.
- [9] D.A. Cremers, L.J. Radziemski, *Handbook of Laser-Induced Breakdown Spectroscopy*, John Wiley & Sons Ltd, USA, 2006.
- [10] C.G. Parigger, J.O. Hornkohl, *Quantum Mechanics of the Diatomic Molecule with Applications*, Institute of Physics (IOP), Bristol, UK, 2019.
- [11] C.G. Parigger, C. M. Helstern, B.S. Jordan, D.M. Surmick, R. Splinter, *Molecules* **25** (2020) 988.
- [12] C.G. Parigger, D.M. Surmick, C. M. Helstern, G. Gautam, A.A. Bol'shakov, R. Russo, Molecular Laser-Induced Breakdown Spectroscopy, Ch. 7 in: *Laser-Induced Breakdown Spectroscopy, 2<sup>nd</sup> ed.*, J.P. Singh, S.N. Thakur, Eds., Elsevier, Amsterdam, NL, 2020, in press.
- [13] M. Dackman, Laser-Induced Breakdown Spectroscopy for Analysis of High Density Methane-Oxygen Mixtures, Master's Thesis, University of Tennessee, Knoxville, TN, 2014.
- [14] H.R. Griem, *Spectral Line Broadening by Plasmas*, Academic Press, New York, USA, 1974.

